



# Long-term warming and interannual variability contributions' to marine heatwaves in the Mediterranean

Amélie Simon<sup>a,\*</sup>, Carlos Pires<sup>a</sup>, Thomas L. Frölicher<sup>b,c</sup>, Ana Russo<sup>a</sup>

<sup>a</sup> Universidade de Lisboa, Faculdade de Ciências, Instituto Dom Luís (IDL), 1749-016 Lisboa, Portugal

<sup>b</sup> Climate and Environmental Physics, Physics Institute, University of Bern, Bern, Switzerland

<sup>c</sup> Oeschger Centre for Climate Change Research, University of Bern, Bern, Switzerland

## ARTICLE INFO

### Keywords:

Marine heatwave  
Mediterranean  
Variability  
Climate change  
Weather pattern  
Air-sea interactions

## ABSTRACT

In the past 40 years, marine heatwaves (MHWs) have experienced a worldwide increase in duration, intensity, frequency and spatial extent. This trend has been particularly evident in the Mediterranean, where exceptional events were observed during the summers of 2022, 2018 and 2003. This study proposes a twofold analysis of MHWs in the Mediterranean, focusing on their statistical characteristics and physical causes. A satellite dataset is utilized to analyze MHWs via an index, called activity, which aggregates the occurrence, duration, intensity and spatial extent of events. Our results show that the trend toward more active summers for MHWs is strongest in the western Mediterranean basin and long-term warming is the main driver in the whole Mediterranean basin. We also show that in the western and Adriatic Mediterranean region, the increase of SST variability contributes about a third to the MHW activity long-term trend whereas in the central, eastern and Aegean basins, the variability of SST mostly acts to diminish this trend. Through principal component analysis (PCA) of MHW activity, we found that the three most severe summer MHW events in the Mediterranean occur at the same location where the overall trend is highest. Interannual variability increased MHW activity in 2022 around the Balearic Sea, in 2018 in the eastern basins and in 2003 in the central basins. A joint PCA revealed that the long-term trend in MHW activity co-varies with a positive geopotential height anomaly over the Mediterranean, which is consistent with the generation of atmospheric-driven MHWs and which, at the North Atlantic scale, resembles the positive phase of the summer East Atlantic. The additional interannual variability contribution to these three severe summers was associated with western warming and projected onto the positive phase of the summer North Atlantic Oscillation. The increase in MHW over the last 40 years is also associated in the western, central and Adriatic regions with increased downward short-wave radiation and in the eastern Mediterranean with decreased upward long-wave radiation. Increased upward latent heat flux partly compensated for the MHW long-term increase over the whole Mediterranean basin. The interannual variability of MHW activity is related in the western, central and Adriatic basins to increased downward sensible and decreased upward latent heat flux possibly due to warm and humid air intrusion.

## 1. Introduction

Marine heatwaves (MHWs) are events of anomalously high sea surface temperature (SST; Hobday et al., 2016). These events can strongly impact marine organisms and socioeconomic systems (e.g., Frölicher and Laufkötter 2018; Smale et al., 2019; Cheung and Frölicher 2020; Smith et al., 2021). Satellite observations over the last four decades have shown that globally MHWs are becoming more frequent and intense, and last longer (Oliver et al., 2018; Frölicher et al., 2018), and that this trend is projected to continue under further global warming (Laufkötter

et al., 2020; Frölicher et al., 2018).

The Mediterranean region, home to 542 million people in 2020 (IPCC report: Ali et al., 2022), warms about 3.7 times faster than the global ocean (Pisano et al., 2020). It is a climate change hotspot due to its high vulnerability and susceptibility to climate risks (Cramer et al., 2018; Cos et al., 2022), including MHWs (Cherif et al., 2020). The warming trend in the Mediterranean over the satellite period, is about  $\sim 0.04$  °C/years (Skliris et al., 2012; Shaltout and Omstedt, 2014; Mohamed et al., 2021; García-Monteiro et al., 2022) and the frequency and intensity of MHWs in the Mediterranean basin is accelerating at a

\* Corresponding author.

E-mail address: [amelie.simon@imt-atlantique.fr](mailto:amelie.simon@imt-atlantique.fr) (A. Simon).

<https://doi.org/10.1016/j.wace.2023.100619>

Received 23 April 2023; Received in revised form 16 October 2023; Accepted 16 October 2023

Available online 23 October 2023

2212-0947/© 2023 The Authors. Published by Elsevier B.V. This is an open access article under the CC BY-NC-ND license (<http://creativecommons.org/licenses/by-nc-nd/4.0/>).

strong pace (Darmaraki et al., 2019a; Simon et al., 2022; Juza et al., 2022; Dayan et al., 2023; Hamdeno and Alvera-Azcaráte, 2023). For example, Pastor and Khodayar (2023) reported a mean annual frequency trend of 3.4 MHW days/year for the period 1982–2021 with strong regional differences; the minimum trend being in the central Mediterranean and the maximum trend being in the northwestern and eastern Mediterranean. Regional differences also exist in MHWs' main features with more frequent and intense MHW in the western Mediterranean and longer events in the eastern Mediterranean (Simon et al., 2022; Hamdeno and Alvera-Azcaráte, 2023).

The top three record MHWs in the Mediterranean in terms of their activity (a single metric combining the occurrence, intensity and duration and spatial extent of these extreme events) in the extended summer over the period 1982–2021 occurred in 2003, 2015 and 2018 (Simon et al., 2022) which is consistent with previous reported severe events (Grazzini and Viterbo, 2003; Garrabou et al., 2009; Bensoussan et al., 2010; Hobday et al., 2018; Darmaraki et al., 2019a; Bensoussan et al., 2019; Ibrahim et al., 2021; Juza et al., 2022). Recently, summer 2022 experienced severe MHWs events in the Mediterranean (Cutroneo and Capello, 2023; González-Alemán et al., 2023; Guinaldo et al., 2023). The rising frequency of MHWs in the Mediterranean is of concern, as previous MHWs have caused changes in structure and mass mortality leading to cascading impacts on fisheries and aquaculture (Galli et al., 2017; Garrabou et al., 2019; Garrabou et al., 2022; IPCC report: Ali et al., 2022). Another consequence of summer MHWs in the Mediterranean is the enhancement of continental heatwaves, reported in 2003 (Feudale and Shukla, 2007; García-Herrera et al., 2010), and the amplification of a severe convective windstorm, documented in 2022 (González-Alemán et al., 2023).

Long-term (or mean) ocean warming is the main driver of the observed increase in MHW frequency at the global scale (Oliver et al., 2018; Frölicher et al., 2018; Xu et al., 2022). However, changes in SST variance or skewness (Alexander et al., 2018; Oliver et al., 2021) due to complex interactions between oceanic and/or atmospheric local and remote processes (Alexander et al., 2018; Holbrook et al., 2019) may also modulate the occurrence of MHW at regional to local spatial scale and at seasonal timescale. In particular in the Mediterranean Sea, Alexander et al. (2018), Oliver et al. (2021), Ciappa (2022) and Xu et al. (2022) found a main role of the mean SST trend in the annual evolution compared to the interannual variability, as found for the global scale. Under future scenarios by 2100, using a fully coupled Regional Climate System Models in the Darmaraki et al. (2019b) estimates that the summer MHW evolution is found to occur mainly due to an increase of the mean SST and about 10–20% due to changes in day-to-day SST variability. However, it is still unclear if the long-term warming contribution to the increase in observed MHWs in summer dominates everywhere in the Mediterranean basin or if changes in SST variability also play a role in some regions. In addition, the contribution of mean warming and interannual variability can differ from one event to another. To the best of our knowledge, no study exists that assesses the contribution of long-term warming and SST variability on single events in the Mediterranean.

There is still little knowledge on how MHWs in the Mediterranean are influenced by large-scale atmospheric variability. Analysis with the SST has demonstrated that the East Atlantic (EA) pattern (Barnston and Livezey, 1987) has a much larger impact on the air–sea heat exchange in the Mediterranean Sea compared to the North Atlantic Oscillation (NAO; Josey et al., 2011). The EA pattern is characterized by a 500 hPa geopotential height (z500) dipole given by a Mediterranean anomalous anticyclone and north-Atlantic-Baltic anomalous depression while the NAO is associated with the strength of the meridional pressure gradient between the Subpolar Low (Island) and the Subtropical (Azores) high (Hurrell et al., 2003). The EA pattern is often interpreted as a southward-shifted NAO pattern. Skliris et al. (2012) indicate a clear positive correlation between the Mediterranean Sea area-averaged long-term warming and the EA index while the decadal SST variability

is associated with the NAO index. Concerning extreme temperature, Hamdeno and Alvera-Azcaráte (2023) find that the annual MHW frequency correlated positively with the EA index in the Mediterranean Sea while the East Atlantic/West Russian index (EATL/WRUS) was strongly negatively correlated with MHW frequency in the eastern Mediterranean basin. The positive phase of the EATL/WRUS is associated with positive height anomalies over Europe and northern China and negative height anomalies over the central North Atlantic and north of the Caspian Sea (Barnston and Livezey, 1987). All these studies have used only a few climate indices to address this question which restricted the number of possibilities. Xoplaki et al. (2003) used a methodology (Canonical correlation analysis between the air surface temperature, taken as predictand and a set of multi-component predictors) that does not assume any climate mode (as they don't use any climate index) to reveal the associated atmospheric circulation (300 hPa geopotential height (z300), 700–1000 hPa thickness) and SST to surface air temperature for extended summers in the period 1950–1999 using detrended monthly data and at  $1^\circ \times 1^\circ$  spatial resolution in the Mediterranean area. Their analysis showed that the first mode exhibits strong positive z300 anomalies centred over Central Europe co-varying with warm surface air temperature and warm SST (maximum in the Central Europe/northwestern Mediterranean basin). Their second mode indicates a negative z300 anomaly centred over the North Sea region covering the northwestern part of the larger Mediterranean area showing a colder area in the western part of the Mediterranean and negative summer air temperature anomalies over Switzerland, France, Spain and Portugal. In this paper, we use a method of the same type of Xoplaki et al. (2003) (joint Principal Component Analysis, see methodology for description) but using higher resolution (daily and  $0.25^\circ \times 0.25^\circ$ ), the period 1982–2022 and used the geopotential height at 500 hPa (z500) and the MHW activity variable to account only for modes that co-varies with extreme oceanic temperature events. In addition, we have used this methodology to reveal the simultaneous connections between MHW activity and air-sea heat fluxes to suggest physical processes generating MHWs.

In this paper, we first analyze how long-term warming and interannual variability of SST influence the long-term summer MHW trend in the Mediterranean over the 1982–2022 period. We then focus on the three most extreme summer MHWs in the Mediterranean Sea (2022, 2018 and 2003) and assess the contributions coming from a long-term evolution and from the interannual variability, using classical Principal Component Analysis (PCA) to reduce dimensionality. We then reveal the atmospheric circulation and fluxes associated with the long-term and interannual contribution of these three events using joint PCA merging oceanic and atmospheric variables.

## 2. Methodology

Daily SST data from the NOAA Optimum Interpolation SST product (OISSTV2; Reynolds et al., 2007; Huang et al., 2020) was used. It is a blend of in-situ data with the satellite sensor Advanced Very High-Resolution Radiometer (AVHRR) data and interpolated at a regular resolution of  $0.25^\circ \times 0.25^\circ$ . The results of our study would need to be further tested with other satellite products but the reconciliation of satellite products is beyond the scope of this study. As we are interested in large-scale MHW, the resolution of OISST ( $0.25^\circ \times 0.25^\circ$ ) is believed to be enough for our purpose. We proceed with OISST as it is widely used for the detection of MHWs (e.g., Hobday et al., 2016; Frölicher et al., 2018; Smale et al., 2019; Ibrahim et al., 2021; Pastor and Khodayar, 2023; Hamdeno and Alvera-Azcaráte, 2023).

Monthly geopotential height at 500 hPa (z500), surface net short-wave radiation flux (SRF), surface net long-wave radiation flux (LRF), surface sensible heat flux (SHF) and surface latent heat flux (LHF) data were obtained from the European Center for Medium-Range Weather Forecasts (ECMWF) reanalysis data ERA5 at a spatial resolution of  $0.25^\circ \times 0.25^\circ$  (Hersbach et al., 2020). We focus on the extended summer

months (JJAS, from 1st of June to 30th of September) of 1982–2022 because it is the season in which the most intense events preferentially occur due to shallow mixed layers and weak winds (Gupta et al., 2020). As SST trends and MHW features can strongly depend on the Mediterranean region (Simon et al., 2022; Juza et al., 2022; Dayan et al., 2023; Pastor and Khodayar, 2023), we define five sub-basins: western, central, eastern, Adriatic and Aegean (see Fig. 7 for the delimitation of these sub-basins).

The detection of MHWs follows a standard approach in which SST exceeds for at least five consecutive days the seasonally varying 90th percentile based on a reference baseline, here the period 1982–2022 (Hobday et al., 2016). The analysis of the spatio-temporal distribution and evolution of MHW is based on the activity index (Simon et al., 2022). The activity is computed at each grid cell for a predefined time range (here the extended summer). The higher the occurrence, duration, intensity and grid cell area is, the higher will be the activity value. It is the sum over every events detected in the time range of the product of their duration, intensity and area of the grid cell and is defined as:

$$Activity = \sum_{EE \cap TimeRange} meanintensity_{EE} \cdot duration_{EE \cap TimeRange} \cdot area_{EE}$$

The EE denotes the discrete (at a given grid cell) extreme events (EE) that occur within the selected time range of analysis;  $meanintensity_{EE}$  (in °C) is the mean temperature anomaly with respect to the climatology; the  $duration_{EE \cap TimeRange}$  (in days) is the duration of the event that remains within the considered time range, and  $area_{EE}$  (in km<sup>2</sup>) is the area affected by the discrete extreme event (that is to say, the grid cell area).

The total activity is a function of time and is the sum of each grid cell activity value within a domain for each considered time range, here summer. By considering all marine events within a predefined domain and time range, this approach generalizes the methodologies considering only events where the daily spatial extent of MHWs in the Mediterranean exceeds 20% in summer (Darmaraki et al., 2019a) or 5% yearly (Pastor and Khodayar, 2023) of the total basin area, and therefore can include MHW of smaller area extent. Based on the same idea as the cumulative intensity which combines the duration and intensity of one event (Hobday et al., 2016), the activity combines the duration and intensity of all area-weighted events over a time range (here the extended summer months).

To split the influences of the long-term (or mean) warming and the interannual variability of SST in the trend of MHW activity (Fig. 2, discussed in the Results section), we take the SST as a nonstationary stochastic process with a drift both in the average and in the shape of the

probability distribution of the anomalies. First, for each spatial coordinate (x,y) in the Mediterranean, we calculate for each extended summer and each year in the period 1982–2022 period, the mean SST, called here  $SST_{full}(t,x,y)$ .

Then, we decompose:

$$SST_{full}(t,x,y) = SST_{trend}(x,y) \cdot t + SST_{anom}(t,x,y)$$

where  $SST_{trend}(x,y) \cdot t$  is the linear trend parcel of SST (coefficient of regression or time slope multiplied by the time in years counted from the beginning of the period),  $SST_{anom}(t,x,y)$  is the anomalous SST with respect to the trend (or detrended SST) which represents the interannual to decadal variability. Then, we compute the regression coefficient of MHW activity from the detected extreme events using  $SST_{anom}(t,x,y)$ , called here  $MHWA_{anom}(x,y)$ . That is the contribution of the SST variability to the MHW activity trend (right panels of Fig. 2). After that, we calculate the regression coefficient of MHW activity from the detected extreme events using  $SST_{full}(t,x,y)$ , called here  $MHWA_{full}(x,y)$  (as in the top-right panel of Fig. 1, discussed in the Results section). Finally, the difference between  $MHWA_{full}(x,y)$  and  $MHWA_{anom}(x,y)$ , called  $MHWA_{trend}(x,y)$  gives the contribution of the mean SST trend to the trend of the MHW activity (left panels of Fig. 2). For the SST, linear regression is used, as it is a good approximation for the long-term warming in the Mediterranean (Pisano et al., 2020; Pastor et al., 2020). A regression of second order was tested for the MHW activity, but the regression is almost fully captured by the first-order coefficient while the second order coefficient is small (not shown). Therefore, the first order coefficient is chosen for the trend of MHW activity. In the supplementary file (Fig. S1), we present a schematic mathematical comparison of the detection of MHW using the full SST and the detrended SST, putting in evidence the effect of a linear trend, either in the mean or in the variance.

One of the components of the study is to contribute to the study of the relationship between MHWs (through the activity index) and large-scale atmospheric circulation (through the z500 field). The circulation at 500 hPa is diagnosed, as this level is commonly used to classify weather patterns in the North Atlantic/European sector (Cassou et al., 2005; Feudale and Shukla, 2007; Folland et al., 2009; Wulff et al., 2017 and many others). To understand how MHWs and atmospheric circulation co-varies, we perform joint (or combined) principal component analysis (JPCA; Kutzbach, 1967). The approach consists of reducing large spatio-temporal datasets from more than one variable (field) to a few dominant time-varying spatial joint patterns (one for each variable) that explain most of the joint variance of the original data. When the number

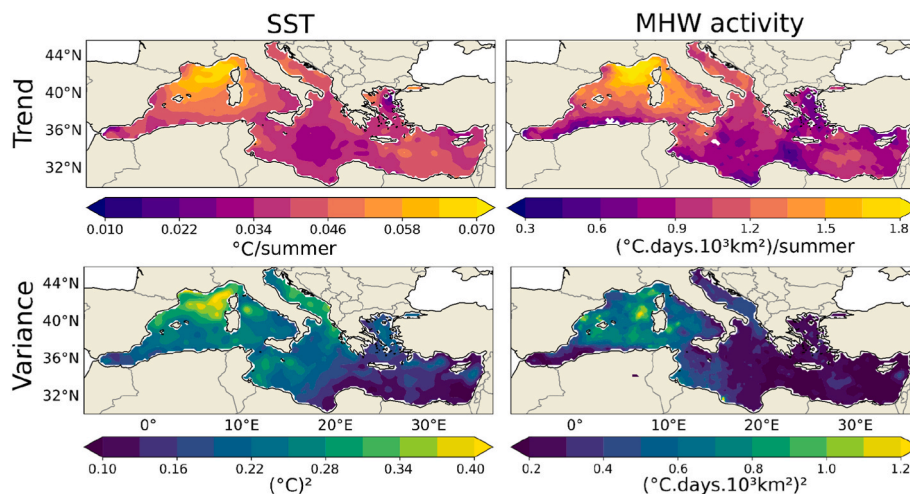
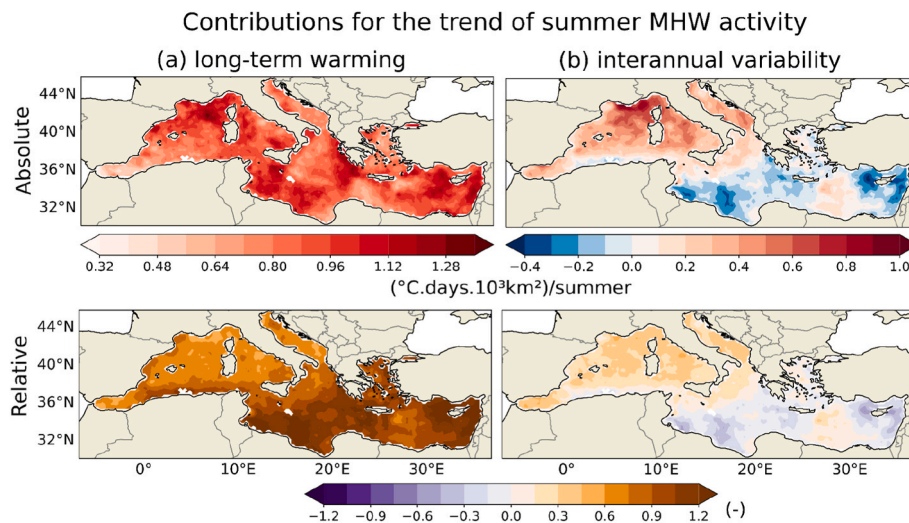


Fig. 1. Summer trend for mean SST (°C/summer; top-left) and MHW activity ((°C.days.10<sup>3</sup>km<sup>2</sup>)/summer; top-right) and variance for detrended SST ((°C)<sup>2</sup>; bottom-left) and detrended MHW activity ((°C.days.10<sup>3</sup> km<sup>2</sup>)<sup>2</sup>; bottom-right) in the Mediterranean over the 1982–2022 period. For the top panels, results are shown only when the trend is significant at 95% using the Mann-Kendall test.



**Fig. 2.** Absolute contribution of long-term warming (or SST mean trend, top-left panel) and interannual SST variability trend (top-right panel) in the total trend of summer MHW activity ( $(^{\circ}\text{C}\cdot\text{days}\cdot 10^3 \text{ km}^2)/\text{summer}$ ). The relative contribution is the respective contribution divided by the full trend of summer MHW activity (obtained with the full SST; bottom panels). The sum of the two relative contributions is one.

of combined fields is two, the JPCA provides nearly the same results as the Maximum Covariance Analysis (MCA; Frankignoul et al., 2011) or the Canonical Correlation Analysis (CCA; Barnston and Ropelewski, 1992) depending on the normalization of data. This JPCA method was used in previous studies to assess the co-variability of pressure, land temperature and land precipitation in the European sector in winter (Fraedrich et al., 1993) and for every season (Casty et al., 2007), or to determine the relationship between rainfall and SST in the Pacific region (Ocampo-Marulanda et al., 2022). Here we assess the co-variability of the z500 and MHW activity as well as the component of air-sea heat fluxes and MHW activity in the Mediterranean in extended summer (JJAS). We also compare this to a similar analysis but with SST or the number of summer MHWs days replacing MHW activity.

To obtain the joint modes, we first reduce dimensionality by performing a PCA (von Storch and Zwiers, 1999) on separately the z500 and MHW activity in the Mediterranean Sea for summer averages (JJAS) over the period 1982–2022 without detrending the variables, thus allowing to include the effect of trend (e.g. long-term warming) in the PCs. We retain ten PCs, of every variable, explaining 97% and 99% of the total (area-integrated) variability, respectively for MHW activity and z500. For the JPCA, we create a single 20-dimensional climate state vector (at every JJAS) concatenating the first ten PCs of each variable (z500 and MHW activity). The PCs have different physical units and variances, so we normalize them by the square root of the total variance of the retained (ten) PCs of each variable in order to preserve the relative importance of each PC. Then, the joint PCA consists of performing a PCA on this 20-component climate state vector over the 41 summers. We then select the leading three joint PCs, explaining 82% of the combined variance (sum of the three leading eigenvalues divided by the sum of all twenty eigenvalues). Then, to obtain how they co-vary with original fields, we compute the corresponding correlation maps, between these joint PCs with on one side the original MHW activity in the Mediterranean basin and on the other side on the z500 in the North Atlantic box (80°W–38°E, 20°N–75°N). In a PCA of a certain field, in a certain target area, and thanks to the PC orthogonality (null correlation between different PCs), the map of the i-th EOF weights and the correlation map between the field and the i-th PC, have the same spatial pattern in the target area (they differ by a multiplicative factor). Similarly, a joint PCA, using the same type of normalization as above, was performed using the MHW activity, short-wave radiation, long-wave radiation, sensible heat flux and latent heat flux. The air-sea heat fluxes are used to have indications of the heat transfer between the ocean and the atmosphere. For

this case, the first four PCs for each variable were used for the joint analysis, explaining respectively 89%, 83%, 84%, 58%, 73% of the respective variance. Table S1 sums up the value of explained variance for all PCAs and JPCAs of this study.

To demonstrate that the joint PCA well captures the covariability, for every joint PC we computed the explained variance of a particular field (e.g. z500 and MHW activity). To do so, and thanks to the PC decorrelation, we computed the fraction of the squared norm of the normalized eigenvector (joint-EOF) corresponding to each field in the state vector used in the joint-PCA. If this fraction is well distributed among the fields, the joint PCs are well mixing the different fields entering the analysis. The fraction of the i-th joint-EOF squared norm multiplied by the i-th fractional joint variance (i-th eigenvalue divided by their overall sum) is the fraction of the explained variance of a particular field by the i-th joint mode. In our case (z500 and MHW activity), that joint-EOF squared norm fraction is the sum of the 10 component squares (first half or second half of the 20-component eigenvector) divided by the sum of the 20 component squares. Table 1 sums up the explained variance of each field for all JPCAs of this study.

### 3. Results

#### 3.1. Evolution and statistical contributors

The mean trend of summer SST is positive in all basins and maximum in the Gulf of Lion-Genoa Gulf area, high in the eastern basin and the

**Table 1**  
Fraction of the squared norm of the normalized eigenvector (joint-EOF) correspondent to each field in the state vector used in the joint-PCA.

		Mode 1	Mode 2	Mode 3
JPCA MHW/z500	MHW activity	0.507	0.492	0.488
	z500	0.493	0.508	0.512
JPCA	SST	0.545	0.461	0.224
SST/z500	z500	0.455	0.539	0.776
JPCA MHW activity/SRF/LRF/SHF/LHF	MHW activity	0.204	0.092	0.387
	SRF	0.246	0.197	0.070
	LRF	0.038	0.562	0.033
	SHF	0.211	0.099	0.316
	LHF	0.300	0.046	0.193

Adriatic Sea, and low in the central basin and Aegean Sea (Fig. 1). These regional trends were also reported for annual values in Mohamed et al. (2021) and in Pastor et al. (2020). By focusing on the eastern/central Mediterranean, Ibrahim et al. (2021) found a stronger trend in the far east compared to the central Mediterranean, also found here. The western Mediterranean accounts for stronger variability in summer detrended SST compared with the eastern region, consistent with García-Monteiro et al. (2022), Hamdeno and Alvera-Azcaráte (2023) and Shaltout and Omstedt (2014); the latter using the coefficient of variation for annual satellite-driven SST from 1982 to 2012. The Gulf of Lion-Genoa Gulf area accounts for the maximum variance of detrended SST.

Using the OISSTV2 product, the estimated annual SST trend for the whole Mediterranean Sea over the 1982–2022 period is  $0.033\text{ }^{\circ}\text{C}/\text{year}$  (not shown), which is on the same order of magnitude as estimated by Mohamed et al. (2021) using the same product for the period 1993–2017 ( $0.036\text{ }^{\circ}\text{C}/\text{year}$ ), by Shaltout and Omstedt (2014) and Pastor et al. (2020) using a product based on the same satellite sensors (AVHRR) to respectively the period 1982–2012 ( $0.035\text{ }^{\circ}\text{C}/\text{year}$ ) and 1982–2019 ( $0.035\text{ }^{\circ}\text{C}/\text{year}$ ), by Skliris et al. (2012) and Pisano et al. (2020) using a higher-resolution reanalysis based on the same satellite respectively during the period 1985–2008 ( $0.037\text{ }^{\circ}\text{C}/\text{year}$ ) and 1982–2018 ( $0.041\text{ }^{\circ}\text{C}/\text{year}$ ), and by García-Monteiro et al. (2022) using the satellite thermal sensor MODIS ( $0.040\text{ }^{\circ}\text{C}/\text{year}$ ). The summer trend estimated here is  $0.042\text{ }^{\circ}\text{C}/\text{summer}$  which is similar to what was found in Skliris et al. (2012) ( $0.044\text{ }^{\circ}\text{C}/\text{summer}$ ) and somewhat smaller than what García-Monteiro et al. (2022) obtained ( $0.070\text{ }^{\circ}\text{C}/\text{summer}$ ). This discrepancy between satellite products is still under debate (López García, 2020; García-Monteiro et al., 2022) and is beyond the scope of this study.

The MHW activity which can be understood as a variable including solely the hot tail of the SST probability distribution with a condition of duration (more than 5 days), shows a generally similar trend in SST mean and variance, although the Adriatic Sea and central Mediterranean basin have relatively smaller MHW variance compared to the one in the SST field. The high summer MHW activity trend can be mainly explained by a trend in more intense and long events in the Gulf of Lion-Genoa Gulf area and mainly longer events in the eastern basin in summer (Simon et al., 2022; Hamdeno and Alvera-Azcaráte, 2023) and is also seen for annual values (Simon et al., 2022; Pastor and Khodayar, 2023). Comparing the trend of summer MHW activity (Fig. 1, top-right panel) with the trend of the number of summer MHW days (Fig. S2) shows both high trend values in the Gulf of Lion-Genoa Gulf area. The trend in the number of summer MHWs days is also high in the southern eastern basin, which is moderate in the MHW activity. Those two regions were also reported by Pastor and Khodayar (2023) for the trend in annual number of MHW days. The differences are explained by the fact that the MHW activity accounts for the trend in intensity, which is stronger for the Gulf of Lion-Genoa Gulf area than for the eastern basin (Simon et al., 2022). Indeed, by using the activity metric, we account for trends in the occurrence, intensity and duration of MHW at each grid cell while the number of MHW days accounts for the duration and occurrence of these events.

For the period 1982–2022, the mean trend in summer SST is  $0.042\text{ }^{\circ}\text{C}/\text{summer}$  and in summer MHW activity is  $1.0\text{ }(^{\circ}\text{C}.\text{days}.10^3\text{ km}^2)/\text{summer}$  (Fig. 1). In Fig. S3, we performed the same analysis as illustrated in Fig. 1 but for two subperiods: 1982–2002 lasting 21 years and 2003–2022 lasting 20 years. These respective subperiods were used as the reference baseline for the detection of MHW which were then used to calculate the MHW activity. We found that the second period has a higher mean trend ( $0.051\text{ }^{\circ}\text{C}/\text{summer}$  for SST and  $1.0\text{ }^{\circ}\text{C}.\text{days}.10^9\text{ m}^2/\text{summer}$  for MHW activity) compared to the first period ( $0.023\text{ }^{\circ}\text{C}/\text{summer}$  for SST and  $4.9\text{ }^{\circ}\text{C}.\text{days}.10^8\text{ m}^2/\text{summer}$  for MHW activity). The fact that the value of the MHW activity trend of the period 2003–2022 is lower than the one for the period 1982–2022 is explained by the different reference baseline to detect the MHWs. Less MHW are detected

during the period 2003–2022 when the reference baseline is 2003–2022 than when the baseline is 1982–2022. As expected for shorter time series, the trends are less significant (for SST and MHW activity). For the first half, only parts of the eastern Mediterranean are significant at 95 % using a Mann-Kendall test. For the second half period, most of the Mediterranean is significant for the SST trend (except the Alboran Sea, Gulf of Gabes and the Adriatic Sea) and MHW activity is significant in the Levantine Sea and Ionian Sea area. Therefore, 20 years are not sufficient to detect a significant trend in SST and MHW activity over the whole Mediterranean (Fig. S3) while for 40 years the trend over the whole Mediterranean is significant (Fig. 1).

The positive trend in MHW activity (Fig. 1, top-right panel) can be due to a shift of the distribution of the mean SST toward warmer states (positive trend of the mean SST) or a widening of the probability density function (PDF) of the SST (a positive trend in the SST variance or other higher order moments, like skewness and kurtosis), thus contributing to thicker PDF ‘hot’ tails. Both causes are consistent with the higher frequency of climatic extremes in a world subjected to global warming (Lewis and King, 2017). Fig. 2 illustrates the absolute and relative contribution of each of the two factors. The relative contribution is the respective contribution divided by the full trend of summer MHW activity (obtained with the full SST; Fig. 2 bottom panels). The sum of the two relative contributions is one. It shows the influences of long-term warming and the interannual variability of SST in the trend of MHW activity (see methodology for the calculation). While long-term warming (or mean SST) contributes to the increase of MHW across the whole basin in a quasi-similar way, temperature variability contributes mostly in the western basin and the Adriatic Sea (Fig. 2, top panels). This contribution of SST variability can be part of the explanation why higher MHW activity is seen in the western basin compared to the rest of the Mediterranean (Fig. 1). In the western basin and the Adriatic Sea, the contribution of the long-term trend is about two-thirds and the interannual variability contribution is about one-third of the total trend in MHW activity (Fig. 2, bottom panels). On the contrary, in the eastern basin, central basin and the Aegean Sea, long-term warming is the main driver of the MHW activity positive trend while the interannual trend is weak or even acts to diminish this positive trend (by reduced SST variability), such as in the central and west Levantine Sea.

To investigate if there is a trend in the contribution of mean SST warming or SST variability changes to MHW activity, we performed the analysis for the two sub-periods 1982–2022 (Fig. S4) and 2003–2022 (Fig. S5). The only common regions where significant total trends (Fig. S3) are found for both subperiods are the Aegean and the east Levantine Seas. In these regions, the main contributor to the long-term trend of MHW activity is the mean warming for both subperiods. The SST variability trend weakly contributes to it in the Aegean Sea and weakly works against it in the east Levantine Sea. Therefore there seems to be no trend in the contributors (mean warming versus variability change) in the significant MHW activity long-term trend.

### 3.2. Severe MHWs summers

Fig. 3 shows the SST, MHW activity and z500 of the three most active summers (JJAS) in terms of MHWs, namely 2022, 2018 and 2003. In 2022, there is a western signature with enhanced activity in the Gulf of Lion-Balearic Sea area, consistent with Cutroneo and Capello (2023), González-Alemán et al. (2023) and Guinaldo et al. (2023). In 2003, there was a western/central signature with strong activity in the Gulf of Lion-Genoa Gulf area, consistent with Skliris et al. (2012) and Pisano et al. (2020). The two extreme summers 2022 and 2003 share a similar pattern with more active MHWs in the western than in the eastern basin while 2018 has a basin-wide signature (except in the Alboran basin).

MHW spatial patterns follow in general the SST anomaly pattern, albeit with some differences. In 2018, maximum SST were localized in the Gulf of Lion-Genoa Gulf area and Aegean Sea while activity shows a more basin-wide signature. In 2022 and 2003, there was enhanced

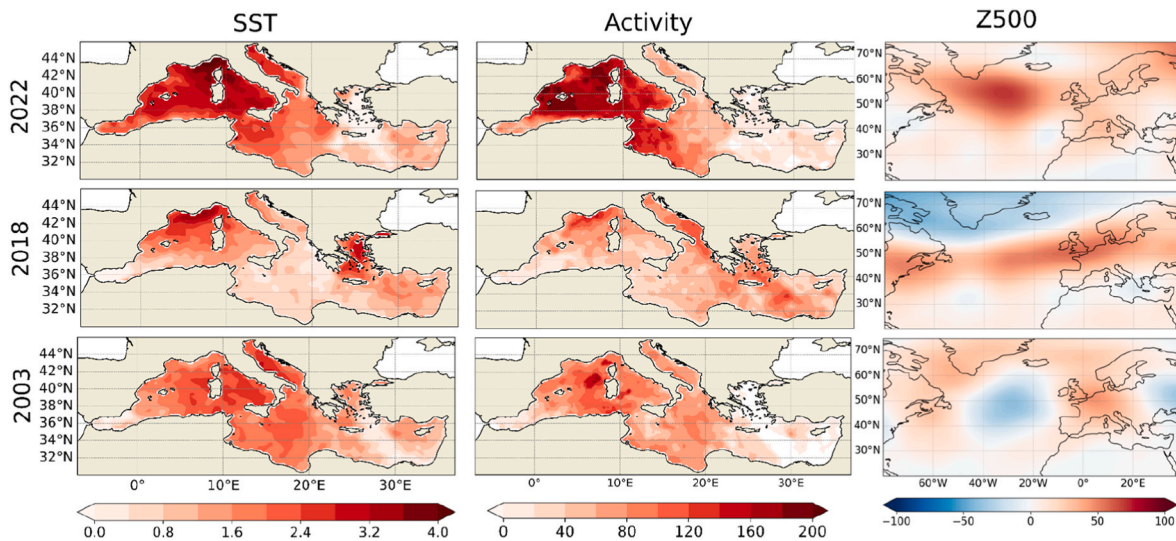


**Fig. 3.** SST anomaly ( $^{\circ}\text{C}$ , left) and geopotential height at 500 hPa (z500) anomaly (m, right) with respect to the summer mean over the period 1982–2022 and MHW activity ( $^{\circ}\text{C}\cdot\text{days}\cdot 10^3 \text{ km}^2$ ; middle) for summer (JJAS) 2022 (top), 2018 (middle), and 2003 (bottom).

MHW activity in the Gulf of Lion-Balearic Sea. As seen in Fig. 1, the Gulf of Lion-Genoa Gulf area corresponds to the region with the highest trend in mean and variance of SST (and of MHW activity), which is consistent with more extreme temperatures and intense MHWs.

The three summers with the highest MHW activity are all associated with dominant z500 positive anomalies in the North Atlantic/European Sector, but the centres of action differ spatially. For the summers of 2022, the centre of action of the height anomaly resides in southern Europe, for summer of 2003 in central Europe and for the summer 2018 in the northern part of Europe. In summer 2022, a strong ridge is also seen in the North Atlantic south of Greenland and west of Great Britain.

### 3.3. PCA analysis

Fig. 4 shows the first three modes (PC time series on the left and map correlation with PCs on the right) of the summer MHW activity calculated with a classical PCA. As expected, an Empirical Orthogonal Function (EOF) weight map shows proportional spatial patterns (Fig. S6) with the map correlation between the PC and the MHW activity (Fig. 4). The first mode of the PCA (Fig. 4) shows a trend associated with an accelerated increase in MHW activity starting from 2000, consistent with the reported intensification in the trend of MHW’s frequency, duration, and intensity since 2000 in the Mediterranean by Pastor and

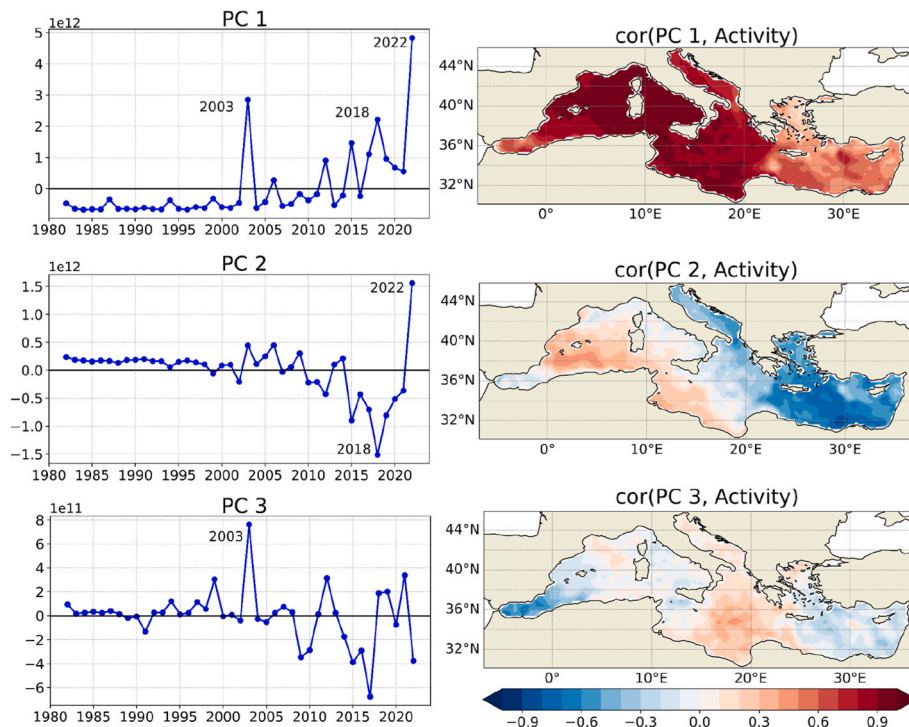


**Fig. 4.** First three principal components (left panels) and correlation maps between the associated PC and MHW activity field (right panels;  $^{\circ}\text{C}\cdot\text{days}\cdot 10^3 \text{ km}^2$ ) over the Mediterranean basin in the summers 1982–2022. Their respectively explained variances by PCs are 72%, 12% and 3%. Note the different ranges of variation of the three PCs. The Mann-Kendall tests at 95% significance show a significant increasing trend for PC 1, a significant decreasing trend for PC 2 and no significant trend for PC 3.

Khodayar (2023). On top of this trend, there are additional large positive peaks for the summers of 2022 followed by 2003 and then 2018 consistent with most reported extreme MHWs (see introduction). Therefore, the three most severe summer MHW events in the Mediterranean occur at the same location where the overall trend is highest (Fig. 4, top-right panel). The increasing trend is significant at 95% using a Mann-Kendall test. The two following modes do not present long-term warming (the second mode shows a significant but weak decreasing trend and the third mode has no significant trend) and therefore their respective PCs are projected mostly onto interannual or decadal variabilities. Therefore, PC 1 is associated with the long-term trend and PC 2 and PC 3 to the variability, which can contain themselves a variability trend. Both in PC 2 and PC 3 time series (Fig. 4), it is apparent an increase of the amplitude of oscillations, especially when comparing the periods 1980–2000 and 2001–2022, thus corroborating a positive trend of the variability intensity (Fig. 1, bottom panels). The second mode is a regional variability mode, showing a west-east Mediterranean contrast in MHW. Its PC 2 shows in the west a slow cooling from 2005 to a minimum in 2018, followed by a sharp warm peak in 2022, whereas in the east the reverse happens. The third mode also reflects a regional mode of interannual variability, especially in the central Mediterranean Sea. The respective PC 3 shows a pronounced warm peak in 2003 and a cold peak in 2017 in the central region.

The MHW signature of summer 2022 (Fig. 3, top-middle panel) was decomposed, mostly as a contribution of long-term warming associated with a basin-wide, maximum in the northwestern warming (PC 1) and as a contribution of interannual variability associated with southwestern warming (PC 2). The MHW activity in the summer of 2018 (Fig. 3, middle panel) is decomposed as a contribution of long-term warming associated with a basin-wide, maximum in the northwestern (PC 1) and as a contribution of interannual variability associated with east/northeast warming, opposite to the summer of 2022 (PC 2). The MHW signature of summer 2003 (Fig. 3, bottom-middle panel) is decomposed as a contribution of long-term warming associated with a basin-wide, maximum in the northwestern (PC 1), and as a contribution of interannual variability associated with central warming (PC 3). Therefore, the three most severe MHWs in the Mediterranean follow the same spatial distribution as the long-term trend. In addition, the interannual variability induces an increase of MHW in 2022 around the Balearic Islands, in 2018 in the eastern Mediterranean and in 2003 in the central Mediterranean.

As expected, these summers (2022, 2018 and 2003) pop up more clearly (larger amplitude in the PCs) than when performing the same analysis with SST (Fig. S7). The correlation of PC 1 on SST and on MHW activity are quite similar in terms of spatial distribution and associated time series, albeit small differences can be seen. In the first mode, more contrast is seen between the western and eastern Mediterranean in the MHW activity variable compared with the SST. One should note that the first three modes on non-seasonal SST (obtained after removing the annual cycle) are similar to those found by Skliris et al. (2012) for the period 1985–2008 using a satellite dataset at a resolution grid of  $1/16^\circ$  over the whole Mediterranean region and for Mohamed et al. (2021) for 1993–2017 and Hamdeno and Alvera-Azcarate (2023) for 1982–2020 using the same satellite product as in this study (OISSTV2 at  $1/4^\circ$  resolution). We also performed the same analysis with the number of summer MHW days instead of the summer MHW activity (Fig. S8). The PCs and correlation maps obtained are mostly similar to using the MHW activity. This is explained by the fact that, in the studied region, the MHW activity mostly reflects the duration of MHWs while the mean intensity of summer MHW presents smaller changes in trend and variability (Simon et al., 2022).

### 3.4. Physical contributors with joint PCA

To reveal the modes where MHWs co-varies with atmospheric circulation, we computed the first three modes of the joint PCA calculated

by including in the same analysis the first ten PCs of MHW activity and the first ten PCs of z500 over the Mediterranean Sea (Fig. 5). The explained variances of the leading first three joint modes are 57%, 18% and 7%, respectively. As expected, correlation maps with z500 are enhanced in the Mediterranean region since the joint analysis is tailored to extract the maximal z500 variance in that region. Table 1 in the supplementary file lists the fractions of each joint-EOF squared norm, corresponding to each field (MHW activity and z500). These fractions are close to 0.5 for joint PC 1 and joint PC 2, showing well-divided variances or equivalently well-mixed joint modes, which is consistent with the higher maximum absolute map correlation values (left and central panels of Fig. 5). The joint PC 3 is mostly projected on z500 (about 78% of the joint-EOF squared norm).

The first mode shows a broadly linear trend starting from 2000 including peaks in 2022, 2018 and 2003 with a western, central and Adriatic regions warming. The atmospheric circulation associated with this long-term warming is a positive z500 anomaly over the Mediterranean. This is consistent with the process of generation of an atmospheric-driven MHW (Vogt et al., 2022), with an anticyclone reducing winds and therefore diminishing the cooling of the SST. This high-pressure system has been reported for the summer of 2003 (Black et al., 2004; Olita et al., 2007; Holbrook et al., 2019). Looking at the large-scale z500 pattern, the first mode resembles the positive phase of the East Atlantic (EA) pattern defined by Barnston and Livezey (1987) and the positive phase of the Summer East Atlantic mode (SEA; Wulff et al., 2017) with a negative height anomaly south of Iceland/west of the British Isles and a positive height anomaly over central Europe/Mediterranean. There are small differences compared to the SEA: the centre of action of the positive height anomaly is slightly too south (expected in northern Europe) and the amplitude of the negative height anomaly is smaller than the positive height anomaly. However, the link between the SEA and temperature is consistent with the one found by Wulff et al. (2017): during a positive phase, a surface air warming over Central Europe and the western Mediterranean is seen in Wulff et al. (2017) and an increase in MHW activity over the whole Mediterranean (maximum in the western Mediterranean) is seen Fig. 5. A similar linkage with the EA has been previously reported for annual values for SST (Josey et al., 2011; Skliris et al., 2012) and MHW frequency (Hamdeno and Alvera-Azcarate (2023).

The second joint mode shows interannual variability, particularly representative of the summer of 2022 with western, central and Adriatic warming and a negative anomalous z500 over the Mediterranean, consistent with a thermodynamic response to surface warming (Kawai et al., 2014), and a positive z500 anomaly in Northern Europe. The z500 projection resembles a positive phase of the summer NAO (Folland et al., 2009), also called a blocking pattern (Cassou et al., 2005). During this phase, anomalous high z500 dominates in northern Europe and anomalous low z500 occurs over Greenland and the Iberian Peninsula/Mediterranean. This is consistent with Skliris et al. (2012) showing a positive correlation between the SST and the NAO index at decadal timescale in the western basin and a negative correlation in the eastern basin. The third mode is similar to the second mode of single EOF with MHW activity (Fig. 4). It shows a contribution of interannual variability for summer 2022 is associated with a diagonal warming/cooling dipole centred over the Mediterranean.

The first three joint modes with z500 and SST (Fig. S9) are quasi-similar to using the activity and z500 (Fig. 5), albeit the peaks are stronger in the activity analysis. Conversely, the second mode presents differences. The second mode of MHW activity shows stronger extreme events in the western, central and Adriatic regions whereas the second mode of SST is basin-wide warming maximum in the eastern basin; both are related with a quasi-similar z500 pattern. Both third modes of SST and MHW activity are similar but the extreme summers do not pop up as clearly with the SST analysis as with the activity analysis. This suggests that analyzing SST or extremely hot SST with a condition of persistence (MHWs) could partly differ for interannual modes.

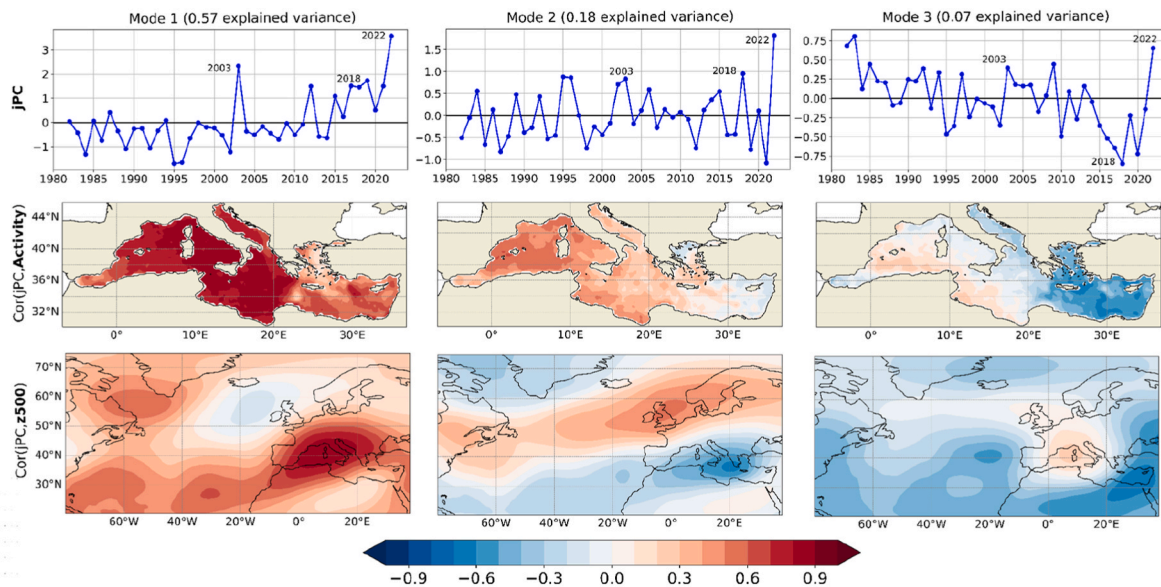


**Fig. 5.** First three joint principal components (PC) obtained with normalized MHW activity and z500 over the Mediterranean basin (top panels), correlation map between the associated PC with the MHW activity (middle panels) and z500 (bottom panels). Their respectively explained variances by PCs are 57%, 18% and 7%. The Mann-Kendall tests at 95% significance show a significantly increasing trend for PC 1, no significant trend for PC 2 and a significantly decreasing trend for PC 3. We caution the reader on the different scales for the y-axis of three PCs.

MHW increases in every location of the Mediterranean (Fig. 1) but the physical process might depend on the region. To better understand the driving mechanism behind the evolution of these MHWs, we performed a joint PCA with 5 variables: the MHWs activity, short-wave radiation, long-wave radiation, sensible heat flux and latent heat flux. Per ECWMF convention, positive fluxes are counted downward. Over the Mediterranean Sea in summer, short-wave radiation and sensible heat fluxes have positive values, and long-wave radiation and latent heat fluxes have negative values. The explained variances of the three first joint modes are 38%, 24% and 12%, respectively. Table 1 lists the fractions of each joint-EOF squared norm, corresponding to each of the five fields. For the first mode, those fractions are well divided (values between 0.2 and 0.3) among MHW activity, short-wave radiation, sensible and latent heat fluxes, whereas the second mode practically captures the covariability between sensible and latent heat fluxes and a small part of MHW act. (0.09). The third mode is mostly projected on the MHW activity, sensible and latent heat fluxes. Like in the joint PCA of MHW activity and z500, larger absolute correlations (in the correlation maps) reflect higher fractional j-EOF squared norms.

In Fig. 6, we show the time evolution of the issuing 3 leading joint PCs (first top row) and respective map-correlations with the 5 target variables (rows 2–6 from the top). The first joint mode (jPC 1) shows a positive linear trend over the 40 years with specifically high positive peaks for 2022 and 2003 (explaining 0.38 of the variance) while the second joint PC (jPC 2) shows a trend starting only around 2010, with a high peak in 2018 (explaining 0.24 of the variance). The third joint mode (jPC 3) at first shows a weak decrease trend until 2010 then a sharp increase (explaining 0.12 of the variance). For this third mode, the summers of 2003 and 2022 have high peaks. The separation between the three modes confirms that 2003 and 2022 are more similar than 2018, even when considering the physical processes in the analysis.

The first mode is highly correlated with positive activity over the whole basin ( $\sim 0.6$ ) except in the Aegean Sea where the correlation falls down to 0.2. Therefore the first mode cannot explain the driving mechanism of MHW generation in the Aegean Sea. In the western, central, and Adriatic regions, the first mode correlates with positive short-wave radiation ( $\sim 0.7$ ) and to a lesser extent to negative latent heat flux ( $\sim -0.5$ ) and negative sensible heat flux ( $\sim -0.4$ ). This means that the increased downward short-wave, the increased upward latent heat

flux and decreased downward sensible heat flux are intimately linked to the MHW mean trend in these regions. This suggests that, in the western, central, and Adriatic regions the main driver of the increase in MHW long-term activity is the increased downward short-wave radiation, warming the ocean, while the increased upward latent fluxes tend to compensate for this upper ocean warming through more cooling (enhanced evaporation as a feedback mechanism). The decreased downward sensible heat flux could be a consequence of reduced winds, leading to less cooling of the upper ocean surface, and would act to warm the ocean, albeit at a lesser extent than shortwave radiation. It could also be a response of a warming SST, leading to a smaller temperature gradient between the air and the ocean, and thus smaller sensible heat flux from the atmosphere to the ocean. This has a cooling action on the ocean trend as less heat from the atmosphere is transferred to the ocean.

In the eastern basin, the MHW activity is mostly correlated with the first and the second joint PCs ( $\sim 0.5$ ) compared with the third ( $\sim 0.1$ ) where the decreased upward long-wave has an important contribution (at the long-term scale and interannual scale). In the Aegean basin, the MHW activity is correlated with the second mode which strongly covaries with decreased upward long-wave radiation. As said previously the second mode mainly reflects the covariability between sensible and latent heat fluxes, and therefore will not be used for interpretation with MHWs activity (Table 1). Therefore, the long-wave radiation seems to be an important factor in the generation of MHW in the eastern basin at long-term timescale. In the first mode, and as for the western, central, and Adriatic regions, MHW activity in the eastern Mediterranean is also associated with increased upward latent heat flux and decreased downward sensible heat flux.

The third mode projects mainly in the MHW activity and sensible and latent heat fluxes (see Table 1) in the western, central and Adriatic basins. The positive correlation between MHW activity and sensible and latent heat fluxes could be explained by warm and humid air intrusion leading to decreased upward latent heat flux (less evaporation) and increased downward sensible heat fluxes (atmosphere warming the ocean).

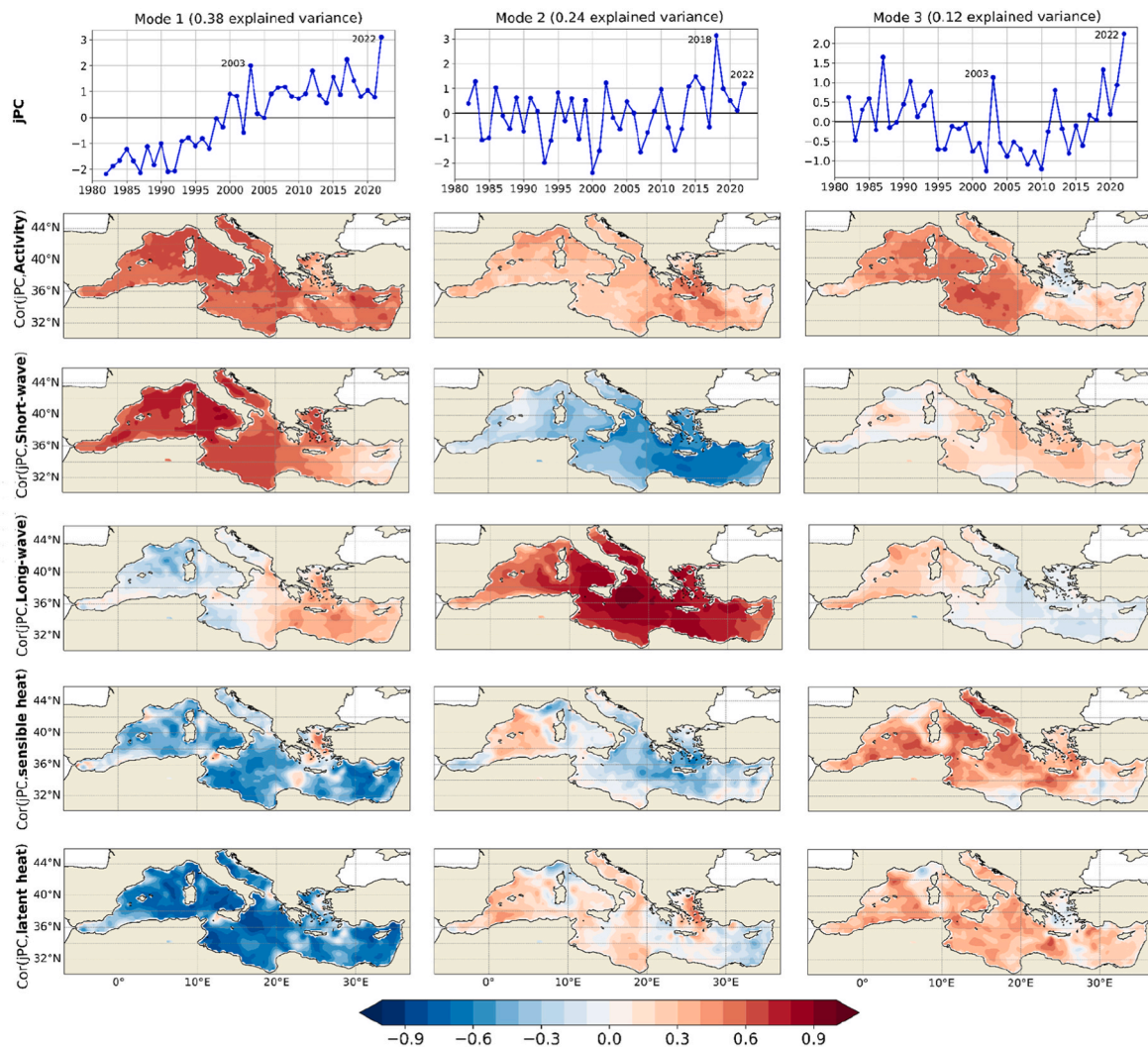


**Fig. 6.** First three joint principal components (jPC; first row from left to right) obtained with normalized MHW activity ( $^{\circ}\text{C}\cdot\text{days}\cdot\text{m}^2$ ), short-wave radiation ( $\text{W}/\text{m}^2$ ), long-wave radiation ( $\text{W}/\text{m}^2$ ), sensible heat flux ( $\text{W}/\text{m}^2$ ) and latent heat flux ( $\text{W}/\text{m}^2$ ). Correlation between the associated jPC with the MHW activity (second row), the short-wave radiation (third row), long-wave radiation (fourth row), sensible heat flux (fifth row) and latent heat flux (sixth). Positive fluxes are downward. The Mann-Kendall tests at 95% significance show a significantly increasing trend for PC 1 and no significant trends for PC 2 and PC 3. We caution the reader on the different scales for the y-axis of three PCs.

#### 4. Discussion and conclusion

Our study addresses the question of what is the contribution of mean warming and interannual variability to the long-term MHW trend in the Mediterranean over the 1982–2022 period using satellite-based data, particularly focusing on the three most extreme summer MHWs in the Mediterranean (2022, 2018 and 2003). Additionally, we investigate the associated atmospheric patterns and heat fluxes.

Consistent with global-scale analyses (Oliver 2019; Oliver et al., 2021; Xu et al., 2022), we found that, over the period 1982–2022, the main driver of the long-term MHW trend is the mean sea surface warming in the whole Mediterranean. This result also stands for projections at the end of the century using global climate models (Alexander et al., 2018) and regional coupled models (Darmaraki et al., 2019b). We also estimate that in the western and Adriatic Mediterranean region, the increase of SST variability contributes up to a third to the MHW long-term trend, whereas in the central, eastern and Aegean basins, the variability of SST acts to diminish it. This latter part is consistent with Xu et al. (2022) as they show that after removing the long-term trend, the MHW occurrences decrease in the eastern Mediterranean. Our estimation in the western and Adriatic Mediterranean region is roughly

consistent with the findings of Xu et al. (2022) as they show a weaker role of the SST variability (compared to the trend) in the MHW duration evolution in this region. By dividing the analysis in two periods (1958–1987 and 1988–2017), they consistently found for three SST datasets (observed, linear inverse model (LIM) and CMIP6) that the non-linear SST trend was responsible not only for the overall shift to warmer values but also for the widening of the distribution, so for the change in SST variability and ultimately to the change in MHWs frequency, while our finding suggests a contribution of about 30% of the SST variability in the long-term evolution of MHWs. This discrepancy could be a reason for the choice of methodologies. While they used a non-linear trend, thus allowing a better estimate for detrending the data and accounting for SST variability, we used a simple linear trend with the assumption that it is well-fitted for your studied period and region (Pisano et al., 2020; Pastor et al., 2020). The difference in the dataset resolution could also explain the contrast in the role of the SST variability. Their use of monthly and  $1^{\circ} \times 1^{\circ}$  resolution data could have filtered some relevant small-scale SST variability compared to our study using daily and  $0.25^{\circ} \times 0.25^{\circ}$  resolution. Seasonality could also be part of the answer, as they used all months and we focused on the summer. The SST variability could be stronger in summer than in other seasons

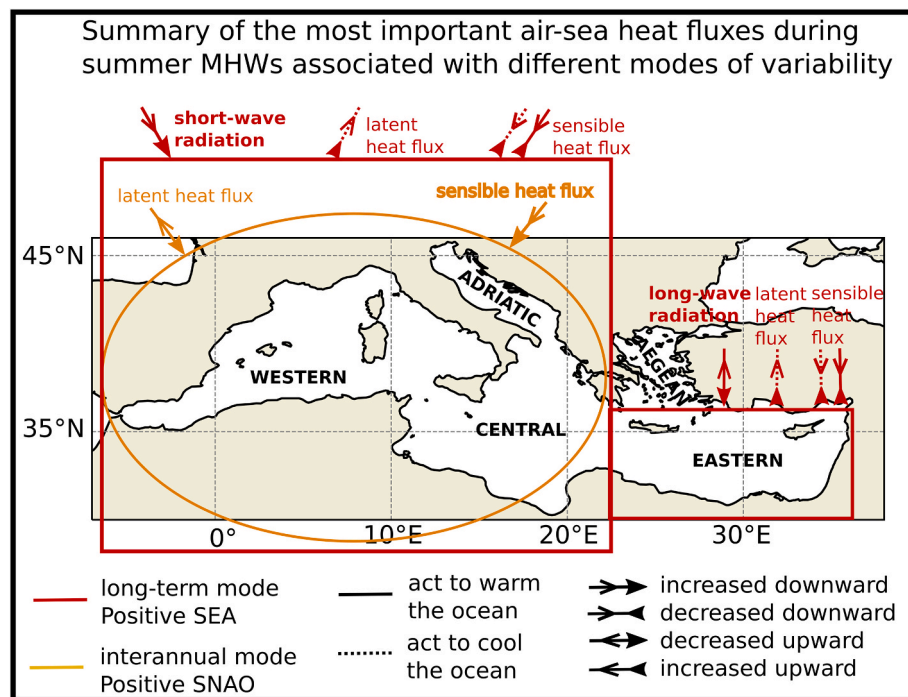


**Fig. 7.** Illustration of the air-sea fluxes and atmospheric circulation associated with the long-term (in red) and interannual (in yellow) evolution of summer MHWs in the Mediterranean over the period 1982–2022. The acronym SEA stands for summer East Atlantic pattern and SNAO for summer North Atlantic Oscillation pattern. These atmospheric patterns are suggested to be linked with respectively the long-term mode and interannual mode. A bold style is used for the dominant air-sea heat flux for each mode. For the long-term mode, it is the short-wave radiation in the western, central and Adriatic basins and long-wave radiation in the eastern basin. For the interannual mode, it is the sensible heat flux in the western, central and Adriatic basins and long-wave radiation in the eastern basin.

due to shallow mixed layer depth allowing a faster surface warming (Juzá et al., 2022). Further study is needed in this direction to quantify the role of the SST variability in the MHW evolution.

A joint PCA revealed that the long-term trend in MHW activity covaries with a positive geopotential height anomaly over the Mediterranean, which is consistent with the generation of atmospheric-driven MHWs and which at the North Atlantic scale resembles the positive phase of the summer East Atlantic pattern. This has shown a certain consistency with previous works using the correlation between the EA index and the SST (Josey et al., 2011; Skliris et al., 2012) or MHW frequency (Hamdeno and Alvera-Azcárate, 2023) in the Mediterranean. Xoplaki et al. (2003) performed a CCA analysis between JJAS anomaly surface air temperatures taken as a predictand and a set of large-scale variables (z300, 700–1000 hPa thickness and SST) taken as predictors. They merged the joint influence of predictands by computing a joint PCA of the predictands only. These joint PCs with the PCs of surface air temperature are then used as inputs for the CCA. The difference with respect to that work is the fact that, instead of taking the full thermal anomaly, we consider the anomaly intensity above a threshold, through the MHW activity, which is taken as input of the JPCA with either z500 or surface heat fluxes. Therefore, the JPCA provides the covariability with oceanic extreme temperatures (marine heatwaves) and not the full anomaly temperatures as in Xoplaki et al., 2003). However, there are some common points as the Mediterranean high-pressure anomaly in the leading mode producing subsidence and surface warming by air compression.

The additional interannual variability contribution to the summers of 2022 and 2003 was associated with western warming and a negative geopotential height anomaly over the Mediterranean, consistent with a thermodynamic response and which resembles the positive phase of the summer NAO. This is consistent with Skliris et al. (2012) showing a positive correlation with the decadal NAO index in the western basin and a negative correlation in the eastern basin. The second mode of Xoplaki et al. (2003) broadly resembles our third mode (diagonal

west/east dipole mode in the Mediterranean in both the ocean and atmospheric field). The positive phase of the summer NAO has been previously shown to be favourable conditions for the generation of MHW at an interannual time scale in the Bay of Biscay and English Channel (Northeastern Atlantic; Simon et al., 2022).

By considering the whole Mediterranean, the long-term increase in MHW activity covaries strongly with the increased upward latent heat fluxes (heat loss from the ocean to the atmosphere). This result shows some consistency with Skliris et al. (2012), which suggests that the long-term SST evolution was mainly driven by latent heat flux variations and with Josey et al. (2011) showing indices of anomalous summer net heat flux with similar impacts on both the eastern and western Mediterranean during the positive phase of the East Atlantic. However, they suggest that radiative fluxes have a smaller contribution to the net heat flux anomalies while we found that they have a dominant role in the long-term evolution of MHWs. This could be explained by the fact that we focus only on summer months. Our method allows the co-variability of multiple variables (short-wave, long-wave, sensible and latent fluxes) at each grid cell. Fig. 7 summarizes our findings related to the air-sea fluxes and atmospheric circulation associated with the long-term and interannual evolution of summer MHWs in the Mediterranean over the period 1982–2022. In the western, central, and Adriatic regions, the main driver of the increase in MHW long-term activity is the increased downward short-wave radiation that warms the upper ocean. The latent heat fluxes tend to compensate for this surface warming through enhanced evaporation. This long-term increase in upward latent heat flux reconciles with the study of Mariotti (2010). With observational water cycle variability datasets, they showed that the long-term changes indicate an overall increase in evaporation during 1958–2006 in the Mediterranean Sea, primarily driven by the SST increase via changes in the surface humidity gradient. The decreased downward sensible heat flux found here could be a consequence of reduced winds, leading to less cooling of the upper ocean surface, and would act to warm the ocean, albeit at a lesser extent than shortwave radiation. It could also be a

response of a warming SST, leading to a smaller temperature gradient between the air and the ocean, and thus smaller sensible heat flux from the atmosphere to the ocean. This has a cooling action on the ocean trend as less heat from the atmosphere is transferred to the ocean.

In the western, central and Adriatic basin, the interannual MHW activity variability, peaking in 2003 and 2022, covaries with decreased upward latent heat fluxes and increased downward sensible (Fig. 6, right panels). This suggests warm air intrusion previously reported for 2003 (Sparnocchia et al., 2006; Olita et al., 2007) and 2022 (Guinaldo et al., 2023) Mediterranean summer MHWs. As the associated MHW activity pattern (Mode 3 of Fig. 6) shows large similarities the MHW activity pattern which covaries with the positive phase of the SNAO (Mode 2 of Fig. 5), we suggest that the positive phase of the SNAO drives the advection of air. This mechanism has been shown by Trigo et al. (2002). Indeed, they found that NAO-related temperature patterns are mainly controlled by the advection of heat by the anomalous mean flow. In the eastern region, the long-term MHW trend coincides mostly with decreased upward long-wave radiation fluxes and, as for the western, central, and Adriatic regions, is also associated with increased upward latent heat flux and decreased downward sensible heat flux. Besides, global climate models have shown that many occurrences of MHWs are associated with increased insolation and reduced ocean heat losses due to high atmospheric pressure and anomalously weak winds (Gupta et al., 2020). Here we showed that the long-term occurrence of MHW is likely driven by greater insolation and decreased downward sensible heat flux which could be explained by reduced winds in the western, central, and Adriatic regions. This last effect could also be due to warming SST, leading to a smaller temperature gradient between the air and the ocean, and thus smaller sensible heat flux from the atmosphere to the ocean. Further investigation would be needed to differentiate these two mechanisms.

Our study has limitations. With observations, we were able to separate the cause of the positive trend of MHW into the increase of the mean of SST and the increase of the variability of SST. However, these contributions mix human influence and natural variability at different time scales. In future studies, the attribution of human influence could be done with the use of climate models (e.g., Frölicher and Laufkötter, 2018; Alexander et al., 2018; Oliver et al., 2021). Besides, the multivariate statistical method applied here (joint PCA) was able to find how the atmosphere co-varies with the MHW in the Mediterranean. We would like to stress that this method does not directly address whether the atmosphere forces or is forced by the ocean (but rather reveals how several variables co-varies), which would call for the assessment of causality diagnostics (Docquier et al., 2023). Although Skliris et al. (2012) claimed that Mediterranean SST spatiotemporal variability is significantly affected by increasing warming from Atlantic inflow, we believe that the ocean current trend would need to be addressed in a future study to have a complete picture of the drivers of the evolution of MHWs. In this sense, climate models could be a useful tool to provide a more mechanistic picture and separate human influence from natural variability. This study aims at better understanding the physical processes involved in the generation of MHWs which may help to better predict these events. The description of the trend and the interannual variability could also give target areas for monitoring these extreme events with subsurface in situ instruments allowing the analysis of vertical propagation of these events.

#### Authors' contribution

AS and CP participated in the conceptual design of the study and of the methodology. AS coded, plotted the figures and wrote the manuscript. Each of the co-authors provided useful insights on the results and a thorough revision of the manuscript.

#### Funding

The authors would like to acknowledge the financial support from Fundação para a Ciência e a Tecnologia, I.P./MCTES through national funds (PIDDAC) – UIDB/50019/2020 – Instituto Dom Luiz and through project ROADMAP (JPIOCEANS/0001/2019). T.L.F was supported by the Swiss National Science Foundation (Grant P00P2\_198897). A.R. was also supported by the Fundação para a Ciência e a Tecnologia, I.P./MCTES through project DHEFEUS (<https://doi.org/10.54499/2022.019185.PTDC>) and grant n°. 2022.01167. CEECIND (COMPLEX).

#### Declaration of competing interest

The authors declare that they have no known competing financial interests or personal relationships that could have appeared to influence the work reported in this paper.

#### Data availability

Data will be made available on request.

#### Acknowledgements

The authors thank Professor Claude Frankignoul for helpful comments on this paper. We thank the two reviewers and the editor for their very helpful and constructive comments.

#### Appendix A. Supplementary data

Supplementary data to this article can be found online at <https://doi.org/10.1016/j.wace.2023.100619>.

#### References

- Alexander, M.A., Scott, J.D., Friedland, K.D., Mills, K.E., Nye, J.A., Pershing, A.J., Thomas, A.C., 2018. Projected sea surface temperatures over the 21st century: changes in the mean, variability and extremes for large marine ecosystem regions of Northern Oceans. *Elementa: Sci. Anthropocene* 6.
- Ali, E., Cramer, W., Carnicer, J., Georgopoulou, E., Hilmi, N.J.M., Le Cozannet, G., Lionello, P., 2022. Cross-chapter paper 4: mediterranean region. In: Pörtner, H.-O., Roberts, D.C., Tignor, M., Poloczanska, E.S., Mintenbeck, K., Alegria, A., Craig, M., Langsdorf, S., Löschke, S., Möller, V., Okem, A., Rama, B. (Eds.), *Climate Change 2022: Impacts, Adaptation and Vulnerability. Contribution of Working Group II to the Sixth Assessment Report of the Intergovernmental Panel on Climate Change*. Cambridge University Press, Cambridge, UK and New York, NY, USA, pp. 2233–2272. <https://doi.org/10.1017/9781009325844.021>.
- Bensoussan, N., Romano, J.C., Harmelin, J.G., Garrabou, J., 2010. High resolution characterization of northwest Mediterranean coastal waters thermal regimes: to better understand responses of benthic communities to climate change. *Estuar. Coast Shelf Sci.* 87 (3), 431–441.
- Barnston, A.G., Livezey, R.E., 1987. Classification, seasonality and persistence of low-frequency atmospheric circulation patterns. *Mon. Weather Rev.* 115 (6), 1083–1126.
- Barnston, A.G., Ropelewski, C.F., 1992. Prediction of ENSO episodes using canonical correlation analysis. *J. Clim.* 5 (11), 1316–1345.
- Bensoussan, N., Chiggiat, J., Buongiorno Nardelli, B., Pisano, A., Garrabou, J., 2019. Insights on 2017 marine heat waves in the Mediterranean Sea. *Copernicus marine service ocean state report, issue 3. J. Oper. Oceanogr.* 12 (suppl. 1), s26–s30. <https://doi.org/10.1080/1755876X.2019.1633075>.
- Black, E., Blackburn, M., Harrison, G., Hoskins, B., Methven, J., 2004. Factors contributing to the summer 2003 European heatwave. *Weather* 59 (8), 217–223.
- Cassou, C., Terray, L., Phillips, A.S., 2005. Tropical Atlantic influence on European heat waves. *J. Clim.* 18 (15), 2805–2811.
- Casty, C., Raible, C.C., Stocker, T.F., Wanner, H., Luterbacher, J., 2007. A European pattern climatology 1766–2000. *Clim. Dynam.* 29 (7), 791–805.
- Cherif, S., Doblas-Miranda, E., Lionello, P., Borrego, C., Giorgi, F., Iglesias, A., Jebari, S., Mahmoudi, E., Moriondo, M., Pringault, O., Rilov, G., Somot, S., Tsikliras, A., Vila, M., Zittis, G., 2020. Drivers of change. In: Cramer, W., Guiot, J., Marini, K. (Eds.), *Climate and Environmental Change in the Mediterranean Basin – Current Situation and Risks for the Future. First Mediterranean Assessment Report. Union for the Mediterranean, Plan Bleu. UNEP/MAP, Marseille, France*, pp. 59–180.
- Cheung, W.W., Frölicher, T.L., 2020. Marine heatwaves exacerbate climate change impacts for fisheries in the northeast Pacific. *Sci. Rep.* 10 (1), 1–10.
- Ciappa, A.C., 2022. Effects of marine heatwaves (MHW) and cold spells (MCS) on the surface warming of the Mediterranean Sea from 1989 to 2018. *Prog. Oceanogr.* 205, 102828.

- Cos, J., Doblas-Reyes, F., Jury, M., Marcos, R., Bretonnière, P.A., Samsó, M., 2022. The Mediterranean climate change hotspot in the CMIP5 and CMIP6 projections. *Earth Syst. Dyn.* 13 (1), 321–340.
- Cramer, W., Guiot, J., Fader, M., Garrabou, J., Gattuso, J.P., Iglesias, A., et al., 2018. Climate change and interconnected risks to sustainable development in the Mediterranean. *Nat. Clim. Change* 8 (11), 972–980.
- Cutroneo, L., Capello, M., 2023. The cold waters in the port of Genoa (NW Mediterranean Sea) during the marine heatwave in summer 2022. *J. Mar. Sci. Eng.* 11 (8), 1568.
- Darmaraki, S., Somot, S., Sevault, F., Nabat, P., 2019a. Past variability of Mediterranean Sea marine heatwaves. *Geophys. Res. Lett.* 46, 9813–9823. <https://doi.org/10.1029/2019GL082933>.
- Darmaraki, S., Somot, S., Sevault, F., Nabat, P., Cabos Narvaez, W.D., Cavicchia, L., et al., 2019b. Future evolution of marine heatwaves in the Mediterranean Sea. *Clim. Dyn.* 53, 1371–1392.
- Dayan, H., McAdam, R., Juza, M., Masina, S., Speich, S., 2023. Marine heat waves in the Mediterranean Sea: an assessment from the surface to the subsurface to meet national needs. *Front. Mar. Sci.* 10, 142.
- Docquier, D., Vannitsem, S., Bellucci, A., 2023. The rate of information transfer as a measure of ocean-atmosphere interactions. *Earth Syst. Dyn.* 14, 577–591. <https://doi.org/10.5194/esd-14-577-2023>.
- Feudale, L., Shukla, J., 2007. Role of Mediterranean SST in enhancing the European heat wave of summer 2003. *Geophys. Res. Lett.* 34 (3).
- Folland, C.K., Knight, J., Linderholm, H.W., Fereday, D., Ineson, S., Hurrell, J.W., 2009. The summer North Atlantic Oscillation: past, present, and future. *J. Clim.* 22 (5), 1082–1103.
- Fraedrich, K., Bantzer, C., Burkhardt, U., 1993. Winter climate anomalies in Europe and their associated circulation at 500 hPa. *Clim. Dynam.* 8 (4), 161–175.
- Frölicher, T.L., Fischer, E.M., Gruber, N., 2018. Marine heatwaves under global warming. *Nature* 560 (7718), 360–364.
- Frölicher, T.L., Laufkötter, C., 2018. Emerging risks from marine heat waves. *Nat. Commun.* 9 (1), 650.
- Frankignoul, C., Chouaib, N., Liu, Z., 2011. Estimating the observed atmospheric response to SST anomalies: maximum covariance analysis, generalized equilibrium feedback assessment, and maximum response estimation. *J. Clim.* 24 (10), 2523–2539. <https://doi.org/10.1175/2010JCLI3696.1>.
- Galli, G., Solidoro, C., Lovato, T., 2017. Marine heat waves hazard 3D maps and the risk for low motility organisms in a warming Mediterranean Sea. *Front. Mar. Sci.* 4 <https://doi.org/10.3389/fmars.2017.00136>.
- García-Herrera, R., Díaz, J., Trigo, R.M., Luterbacher, J., Ficher, E., 2010. A review of the European summer heat wave of 2003. *Crit. Rev. Environ. Sci. Technol.* 40, 267–306.
- Garrabou, J., Gómez-Gras, D., Ledoux, J.B., Linares, C., Bensoussan, N., et al., 2019. Collaborative database to track mass mortality events in the Mediterranean Sea. *Front. Mar. Sci.* 6, 707. <https://doi.org/10.3389/fmars.2019.00707>.
- García-Monteiro, S., Sobrino, J.A., Julien, Y., Soria, G., Skokovic, D., 2022. Surface Temperature trends in the Mediterranean Sea from MODIS data during years 2003–2019. *Reg. Stud. Mar. Sci.* 49, 102086.
- Garrabou, J., Coma, R., Bensoussan, N., Bally, M., Chevaldonné, P., Cigliano, M., et al., 2009. Mass mortality in Northwestern Mediterranean rocky benthic communities: effects of the 2003 heat wave. *Global Change Biol.* 15 (5), 1090–1103.
- Garrabou, J., Gómez-Gras, D., Medrano, A., Cerrano, C., Ponti, M., Schlegel, R., et al., 2022. Marine heatwaves drive recurrent mass mortalities in the Mediterranean Sea. *Global Change Biol.* 28 (19), 5708–5725. <https://doi.org/10.1111/gcb.16301>.
- Grazzini, F., Viterbo, P., 2003. Record-breaking warm sea surface temperature of the Mediterranean Sea. *ECMWF Newsletter* 98, 30–31.
- González-Alemán, J.J., Insua-Costa, D., Bazile, E., González-Herrero, S., Marcello Miglietta, M., Groenemeijer, P., Donat, M.G., 2023. Anthropogenic warming had a crucial role in triggering the historic and destructive mediterranean derecho in summer 2022. *Bull. Am. Meteorol. Soc.* 104 (8), E1526–E1532.
- Guinaldo, T., Voldoire, A., Waldman, R., Saux Picart, S., Roquet, H., 2023. Response of the sea surface temperature to heatwaves during the France 2022 meteorological summer. *Ocean Sci.* 19 (3), 629–647.
- Gupta, A.S., Thomsen, M., Benthuyssen, J.A., Hobday, A.J., Oliver, E., Alexander, L.V., et al., 2020. Drivers and impacts of the most extreme marine heatwave events. *Sci. Rep.* 10 (1), 1–15.
- Hamdeno, M., Alvera-Azcara, A., 2023. Marine heatwaves characteristics in the Mediterranean Sea: case study the 2019 heatwave events. *Front. Mar. Sci.* 10, 1093760. <https://doi.org/10.3389/fmars.2023.1093760>.
- Hersbach, H., Bell, B., Berrisford, P., Hirahara, S., Horányi, A., Muñoz-Sabater, J., et al., 2020. The ERA5 global reanalysis. *Q. J. R. Meteorol. Soc.* 146 (730), 1999–2049 (Accessed on 03-10-2022).
- Hobday, A.J., Alexander, L.V., Perkins, S.E., Smale, D.A., Straub, S.C., Oliver, E.C., et al., 2016. A hierarchical approach to defining marine heatwaves. *Prog. Oceanogr.* 141, 227–238.
- Hobday, A.J., Oliver, E.C.J., Sen Gupta, A., Benthuyssen, J.A., Burrows, M.T., Donat, M.G., Holbrook, N.J., Moore, P.J., Thomsen, M.S., Wernberg, T., Smale, D.A., 2018. Categorizing and naming marine heatwaves. *Oceanography* 31 (2), 162–173. <https://doi.org/10.5670/oceanog.2018.205>.
- Holbrook, N.J., Scannell, H.A., Sen Gupta, A., Benthuyssen, J.A., Feng, M., Oliver, E.C.J., Alexander, L.V., Burrows, M.T., Donat, M.G., Hobday, A.J., Moore, P.J., Perkins-Kirkpatrick, S.E., Smale, D.A., Straub, S.C., Wernberg, T., 2019. A global assessment of marine heatwaves and their drivers. *Nat. Commun.* 10 (1) <https://doi.org/10.1038/s41467-019-10206-z>.
- Huang, B., Liu, C., Banzon, V., Freeman, E., Graham, G., Hankins, B., Smith, T., Zhang, H.-M., 2020. Improvements of the daily Optimum interpolation sea surface temperature (DOISST) version 2.1. *J. Clim.* 34, 2923–2939. <https://doi.org/10.1175/JCLI-D-20-0166> (Accessed on 03-10-2022).
- Hurrell, J.W., Kushnir, Y., Otttersen, G., Visbeck, M., 2003. An overview of the North Atlantic oscillation. *Geophys. Monogr.-Am. Geophys. Union* 134, 1–36.
- Ibrahim, O., Mohamed, B., Nagy, H., 2021. Spatial variability and trends of marine heat waves in the eastern mediterranean sea over 39 years. *J. Mar. Sci. Eng.* 9 (6), 643.
- Josey, S.A., Somot, S., Tsimplis, M., 2011. Impacts of atmospheric modes of variability on Mediterranean Seasurface heat exchange. *J. Geophys. Res.* 116, C02032 <https://doi.org/10.1029/2010JC006685>.
- Kutzbach, J.E., 1967. Empirical eigenvectors of sea-level pressure, surface temperature and precipitation complexes over North America. *J. Appl. Meteorol. Climatol.* 6 (5), 791–802.
- Juza, M., Fernández-Mora, À., Tintoré, J., 2022. Sub-Regional marine heat waves in the Mediterranean Sea from observations: long-term surface changes, Sub-surface and coastal responses. *Front. Mar. Sci.* 9, 785771.
- Kawai, Y., Tomita, H., Cronin, M.F., Bond, N.A., 2014. Atmospheric pressure response to mesoscale sea surface temperature variations in the Kuroshio Extension: in situ evidence. *J. Geophys. Res.* 119, 8015–8031.
- Laufkötter, C., Zscheischler, J., Frölicher, T.L., 2020. High-impact marine heatwaves attributable to human-induced global warming. *Science* 369 (6511), 1621–1625.
- Lewis, S.C., King, A.D., 2017. Evolution of mean, variance and extremes in 21st century temperatures. *Weather Clim. Extrem.* 15, 1–10.
- López García, M.J., 2020. SST comparison of AVHRR and MODIS time series in the western Mediterranean Sea. *Rem. Sens.* 12 (14), 2241.
- Mariotti, A., 2010. Recent changes in the Mediterranean water cycle: a pathway toward long-term regional hydroclimatic change? *J. Clim.* 23 (6), 1513–1525.
- Mohamed, B., Nagy, H., Ibrahim, O., 2021. Spatiotemporal variability and trends of marine heat waves in the red Sea over 38 years. *J. Mar. Sci. Eng.* 9 (8), 842.
- Ocampo-Marulanda, C., Fernández-Álvarez, C., Cerón, W.L., Canchala, T., Carvajal-Escobar, Y., Alfonso-Morales, W., 2022. A spatiotemporal assessment of the high-resolution CHIRPS rainfall dataset in southwestern Colombia using combined principal component analysis. *Ain Shams Eng. J.* 13 (5), 101739.
- Olita, A., Sorgente, R., Natale, S., Gaberšek, S., Ribotti, A., Bonanno, A., Patti, B., 2007. Effects of the 2003 European heatwave on the Central Mediterranean Sea: surface fluxes and the dynamical response. *Ocean Sci.* 3, 273–289. <https://doi.org/10.5194/os-3-273-2007>.
- Oliver, E.C., Donat, M.G., Burrows, M.T., Moore, P.J., Smale, D.A., Alexander, L.V., et al., 2018. Longer and more frequent marine heatwaves over the past century. *Nat. Commun.* 9 (1), 1–12.
- Oliver, E.C., 2019. Mean warming not variability drives marine heatwave trends. *Clim. Dyn.* 53 (3–4), 1653–1659.
- Oliver, E.C., Benthuyssen, J.A., Darmaraki, S., Donat, M.G., Hobday, A.J., Holbrook, N.J., et al., 2021. Marine heatwaves. *Ann. Rev. Mar. Sci.* 13, 313–342.
- Pastor, F., Valiente, J.A., Khodayar, S., 2020. A warming mediterranean: 38 Years of increasing sea surface temperature. *Rem. Sens.* 12, 2687. <https://doi.org/10.3390/rs12172687>.
- Pastor, F., Khodayar, S., 2023. Marine heat waves: characterizing a major climate impact in the Mediterranean. *Sci. Total Environ.*, 160621.
- Pisano, A., Marullo, S., Artale, V., Falcini, F., Yang, C., Leonelli, F.E., et al., 2020. New evidence of Mediterranean climate change and variability from sea surface temperature observations. *Rem. Sens.* 12 (1), 132.
- Reynolds, R.W., Smith, T.M., Liu, C., Chelton, D.B., Casey, K.S., Schlax, M.G., 2007. Astor Daily high-resolution-blended analyses for sea surface temperature. *J. Clim.* 20, 5473–5496.
- Shaltout, M., Omstedt, A., 2014. Recent sea surface temperature trends and future scenarios for the Mediterranean Sea. *Oceanologia* 56 (3), 411–443.
- Simon, A., Plecha, S.M., Russo, A., Teles-Machado, A., Donat, M.G., Auger, P.-A., Trigo, R.M., 2022. Hot and cold marine extreme events in the Mediterranean over the period 1982–2021. *Front. Mar. Sci.* 9, 892201.
- Skliris, N., Sofianos, S., Gkanasos, A., Mantziafou, A., Vervatis, V., Axaopoulos, P., Lascaratos, A., 2012. Decadal scale variability of sea surface temperature in the Mediterranean Sea in relation to atmospheric variability. *Ocean Dyn.* 62, 13–30.
- Smale, D.A., Wernberg, T., Oliver, E.C., Thomsen, M., Harvey, B.P., Straub, S.C., et al., 2019. Marine heatwaves threaten global biodiversity and the provision of ecosystem services. *Nat. Clim. Change* 9 (4), 306–312.
- Smith, K.E., Burrows, M.T., Hobday, A.J., Sen Gupta, A., Moore, P.J., Thomsen, M., et al., 2021. Socioeconomic impacts of marine heatwaves: global issues and opportunities. *Science* 374 (6566), eabj3593.
- Sparnocchia, S., Schiano, M.E., Picco, P., Bozzano, R., Cappelletti, A., 2006. The anomalous warming of summer 2003 in the surface layer of the Central Ligurian Sea (Western Mediterranean). *Ann. Geophys.* 24 (2), 443–452. Copernicus GmbH.
- Trigo, R.M., Osborn, T.J., Corte-Real, J.M., 2002. The North Atlantic Oscillation influence on Europe: climate impacts and associated physical mechanisms. *Clim. Res.* 20 (1), 9–17.
- Vogt, L., Burger, F.A., Griffies, S.M., Frölicher, T.L., 2022. Local drivers of marine heatwaves: a global analysis with an earth system model. *Front. Clim.* 49.
- von Storch, H., Zwiers, F.W., 1999. *Statistical Analysis in Climate Research*. Cambridge University Press, p. 484. <https://doi.org/10.1017/CBO9780511612336>.
- Wulff, C.O., Greatbatch, R.J., Domeisen, D.I.V., Gollan, G., Hansen, F., Tropical, 2017. Forcing of the Summer East atlantic pattern. *Geophys. Res. Lett.* 44 <https://doi.org/10.1002/2017GL075493>, 166–111.
- Xoplaki, E., González-Rouco, J.F., Luterbacher, J., Wanner, H., 2003. Mediterranean summer air temperature variability and its connection to the large-scale atmospheric circulation and SSTs. *Clim. Dyn.* 20, 723–739.
- Xu, T., Newman, M., Capotondi, A., Stevenson, S., Di Lorenzo, E., Alexander, M.A., 2022. An increase in marine heatwaves without significant changes in surface ocean temperature variability. *Nat. Commun.* 13 (1), 7396.